Concentration Fluctuations in Sheared Polymer Solutions

Hong Ji and Eugene Helfand*

AT&T Bell Laboratories, Murray Hill, New Jersey 07974

Received August 25, 1994; Revised Manuscript Received February 10, 1995[⊗]

ABSTRACT: When subjected to shear flow, polymer solutions can exhibit strongly enhanced concentration fluctuations, leading to an observed increase in light scattering with a characteristic angular dependence. This is attributable to the coupling of polymer concentration to the polymer elastic stress. We have developed a phenomenological model to study the polymer concentration fluctuations in the presence of flow. We use the two-fluid model (separate polymer and solvent flow fields) to obtain Langevin equations for concentration, velocity, and a defined polymer strain. The constitutive equation employed is a simplified Doi–Edwards model derived from reptation theory. We will present results for the structure factor under steady-state shear for scattering wave vectors in the q_xq_y and q_xq_z planes, where x = flow direction, y = gradient direction, and z = vorticity direction. The results are compared with scattering measurements. We have also studied the effects of a small oscillatory shear added to the steady shear.

I. Introduction

Polymer solutions exhibit an increase in turbidity when rapidly sheared, e.g., when forced through a capillary.[1] Recently, Helfand and Fredrickson[2] (HF) proposed a mechanism to explain this phenomenon. They argue that the observed turbidity is a consequence of enhanced concentration fluctuations caused by the coupling between polymer concentration fluctuations and polymer elastic stress under shear. In particular, their hydrodynamic model predicted an overall enhanced but highly anisotropic structure factor which could be measured in light scattering experiments. These experiments were subsequently carried out by several groups,[3–5] and the observed "butterfly" scattering patterns were in qualitative agreement with the HF model.

However, several features of the observed scattering patterns were not fully accounted for. For example, one important feature (which gives the name "butterfly" to the patterns) is the appearance of two symmetric peaks at finite wave vectors in the scattering patterns. The peak position corresponds to the so-called "magic length"[6] defined as the crossover between two relaxational rates in entangled polymer solutions, namely, concentration diffusion and stress relaxation. This suggestive feature actually revealed why the HF model failed to predict the existence of the peaks. In the HF model, stress was assumed to relax rapidly to a value consistent with the local, fluctuating concentration.[2] In order to understand fully the light scattering results, a complete hydrodynamic theory that addresses the issue of stress dynamics is needed.

Onuki[7] and Milner[8] used a phenomenological approach to write down a coupled set of Langevin equations for polymer concentration, velocity, and polymer strain. Several physical models were used in order to determine the unknown phenomenological parameters in the Langevin equations. One is the two-fluid model of polymer plus solvent, introduced by Brochard and de Gennes[6] in their study of the dynamics of entangled polymer solutions. This model makes manifest the coupling between polymer concentration and polymer elastic stress. As is shown in the HF work, this is precisely what leads to the enhancement of polymer concentration fluctuations under shear.

Using this approach, Milner[8] calculated the nonequilibrium structure factors $S(\mathbf{q})$ in the limit of weak shear. The scattering wave vector, $\mathbf{q}$, was considered to be in the q_xq_y plane defined by the velocity (x) and the gradient (y) directions. The calculated $S(\mathbf{q})$ agrees qualitatively with the rotating "butterfly" scattering patterns observed by Wu *et al.*[3] Since the calculation was carried out only to the first order of the shear rate, the interesting effects at high shear rate (including shear thinning and normal stresses)[9] were not properly represented.

In this paper, we present a full calculation of the polymer structure factor using the phenomenological approach similar to that of Onuki and Milner. The constitutive equation is a simplified Doi–Edwards model derived from the reptation theory.[10] The resulting constitutive equation shows shear thinning and first and second normal stresses. The structure factor $S(\mathbf{q})$ is calculated for arbitrary $\mathbf{q}$ vectors. To compare with experiments, we present here the results for $\mathbf{q}$ vector confined to the q_xq_y and q_xq_z planes, respectively (x = flow direction, y = velocity gradient direction, z = vorticity direction).

This paper is organized as follows. In section II we present a physical description of shear-induced fluctuations in polymer solutions. This is followed by a discussion of the two-fluid model. In sections IV and V, we derive the Langevin equations for polymer concentration, velocity, and a defined polymer strain. These equations are used in sections VI and VII to study fluctuations in polymer solutions under steady shear. In section VIII, we study the effect of non-steady shear by adding an oscillatory component to the steady shear. In section IX, we describe the numerical method used in calculating the nonequilibrium polymer structure factor. The results are compared with existing experimental data in section X, where we conclude with a discussion of the limitations and possible extensions of the present model.

II. Physical Description

We begin with a physical description of the processes that lead to shear-induced fluctuations, as predicted by HF. Consider a semidilute polymer solution. The polymer concentration field can change in two ways. The first is by diffusion of the polymer mass, with a diffusion constant inversely proportional to the friction constant. The second is by unbalanced elastic forces pulling the

[⊗] Abstract published in *Advance ACS Abstracts,* May 1, 1995.

0024-9297/95/2228-3869$09.00/0

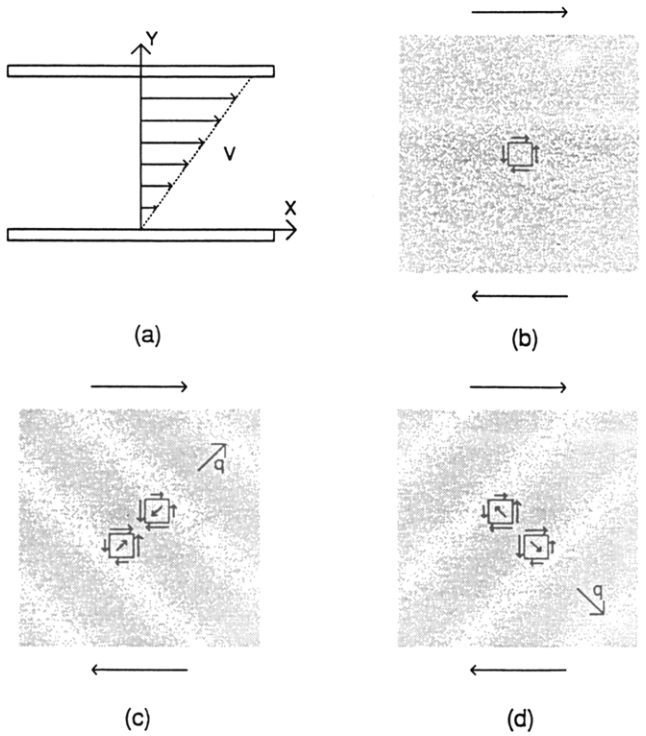

Figure 1. (a) Schematic illustration of the velocity field in simple shear, $\mathbf{v} = \dot{\gamma} y \mathbf{e}_x$. (b) Shear forces exerted on the surfaces of a volume element in a uniform system. (c) A concentration wave, with wave vector in the direction of $q_x = q_y$ in the shear field. Surface forces and the net forces on the volume elements are indicated as arrows. For this wave, net shear force tends to move polymers to a more concentrated region, opposing diffusion. (d) A concentration wave, with wave vector in the direction of $q_x = -q_y$. Here shear force tends to move polymers away from the more concentrated region, aiding diffusion.

polymer. Let us be a bit more detailed about the latter, since it is less familiar. Consider a polymer solution in simple shear, with the velocity in direction x and the gradient in direction y (Figure 1a). On average this sets up stresses on each element, and in Figure 1b we illustrate the tangential (off diagonal) forces exerted in uniform shear by the material outside a volume element on the material inside (i.e., stresses). Note the balance of the xy and the yx components of the stress, leading to no net torque. Also opposite faces have equal and opposite forces, corresponding to the fact that the stress is assumed to be uniform. The result is that for a uniform system there is no net force on the volume element. Next consider a system where the stress is not uniform. We will focus on a case where this arises as a result of there being a concentration wave in the system. We have in mind that the concentration wave is a component of some spontaneous concentration fluctuation. Because viscosity varies strongly with concentration in a polymer system, one finds that the stress is higher in the high-concentration region. The boundary forces on a volume element are as illustrated by the arrows in Figure 1c. The two surfaces located in the more concentrated region experience higher forces than the forces on the two boundaries located in the less concentrated region. For a concentration wave in the direction defined by $q_x = q_y$ (Figure 1c), there is a net force on the polymer within the element pulling it into the region of higher concentration. The effect is the opposite of diffusion. Thus the dissipation of this concentration wave becomes slower, or can even turn into a growth. As will be seen in detail in a later section, this wave is convected, eventually, so that the wave vector points in a direction where the dissipation dominates. This avoids a runaway growth.

The effect of polymer stress clearly depends on the directions of concentration fluctuation waves. For example, in the direction defined by $q_x = -q_y$, a concentration wave tends to decay faster. In this case inhomogeneous polymer stress works along with diffusion to smooth out concentration inhomogeneities (Figure 1d). Generally speaking, concentration waves with wave vectors in the first (or third) quadrant are being enhanced by this mechanism, and those with wave vectors in the second (or fourth) quadrant are diminishing (but we shall see that this is not always the case). The result is a highly anisotropic distribution in the intensity of concentration fluctuations that can be probed by scattering experiments. This argument can be easily generalized to understand the effects of normal stresses.

There exists an implicit assumption in the HF mechanism discussed qualitatively above. Polymer stress is assumed to follow rapidly the variations in local concentration. One knows that concentration fluctuations dissipate by diffusion at a rate given by Dq^2, while stress has characteristic rate of change $1/\tau$ independent of q (for entangled polymers τ is the reptation time). Therefore, for small enough q the assumption that stress response is the faster process will always be valid. However, light (or X-rays or neutrons) can easily probe values of q large enough that the assumption breaks down. Let us define a characteristic magnitude for a wave vector, q^*, corresponding to the crossover of time scales, $Dq^{*2} = 1/\tau$. The HF mechanism loses effectiveness, and the scattering decreases for larger $q \gtrsim q^*$.

This was evident already in the first studies, by Wu, Pine, and Dixon,[3] of anisotropic scattering from a polymer solution under shear. (The above physical explanation was attributed therein to Milner.[8]) That study and more recent light scattering experiments[3,4] show anisotropically enhanced light scattering in the low-q region, with peaks located at wavenumbers where diffusion rate is comparable to stress relaxation rate.

III. The Two-Fluid Model

To establish a theoretical framework for these physical considerations, HF showed[2] that the crucial stress–concentration coupling emerged from the microscopic chain dynamics in the context of the Rouse model. Doi[11] and Milner[8] have developed an insightful, and more general, way to derive the fundamental equations of the theory. They employ the two-fluid model of Brochard and de Gennes.[6] We review that approach here.

Let ϕ be the polymer concentration as a volume fraction, and $\mathbf{v}_p$ and $\mathbf{v}_s$ the velocities for polymer and solvent, respectively. Let ϱ_{0p} and ϱ_{0s} be the mass densities for pure polymer and solvent, respectively. The equation of motion for polymer concentration is given by conservation of mass:

$$\frac{\partial \phi}{\partial t} = -\nabla\cdot(\phi \mathbf{v}_p) \tag{1}$$

A small volume element of polymer experiences the following forces: (1) osmotic force, $-\nabla\pi_\phi$; (2) force due to inhomogeneity in polymer elastic stress, $\nabla\cdot\boldsymbol{\sigma}_p$; and (3) friction due to the relative motions between polymer and solvent, $\lambda(\mathbf{v}_s - \mathbf{v}_p)$. For a small volume element of solvent, the forces experienced are (1) solvent viscous force, $\eta_s\nabla^2\mathbf{v}_s$; (2) hydrostatic force, ∇p; and (3) friction

due to the relative motion between polymer and solvent, $-\lambda(\mathbf{v}_s - \mathbf{v}_p)$. The momentum equations for polymers and solvents are then

$$\varrho_{0p}\phi\frac{\partial \mathbf{v}_p}{\partial t} = -\nabla\pi_\phi + \nabla\cdot\boldsymbol{\sigma}_p + \lambda(\mathbf{v}_s - \mathbf{v}_p) \tag{2}$$

$$\varrho_{0s}(1-\phi)\frac{\partial \mathbf{v}_s}{\partial t} = \eta_s\nabla^2\mathbf{v}_s - \nabla_p - \lambda(\mathbf{v}_s - \mathbf{v}_p) \tag{3}$$

Here η_s is the solvent viscosity. The parameter λ is the drag coefficient, which describes friction between polymer and solvent. It is given by[6] $\lambda \simeq \eta_s/\xi^2$, where ξ is the excluded volume screening length (assumed proportional to the hydrodynamic screening length).[12] We neglected momentum convection terms since the Reynolds numbers involved are usually low.[13] We also made use of the fact that in semidilute polymer solutions $\phi \ll 1$.

Due to their small volume fraction, polymers in semidilute solutions have low inertia, causing them to follow quickly the motion of the ambient solvent under the action of large drag forces. Consequently, polymer velocity relaxes much faster than the solvent velocity in semidilute polymer solutions. We may therefore neglect the inertial term in eq 2 and express the polymer velocity in terms of the solvent velocity and other variables via the following relation:

$$\mathbf{v}_p = \mathbf{v}_s + \lambda^{-1}(-\nabla\pi_\phi + \nabla\cdot\boldsymbol{\sigma}_p) \tag{4}$$

The solvent velocity may be equated to the total fluid velocity, $\mathbf{v}$, and solvent density to fluid density, ϱ, because the contribution of the polymer is negligibly small for small ϕ. In terms of the new velocity variable, we have

$$\mathbf{v}_p = \mathbf{v} + \mathbf{v}' \tag{5}$$

where $\mathbf{v}'$ describes the lagging of polymer velocity

$$\mathbf{v}' = \lambda^{-1}(-\nabla\pi_\phi + \nabla\cdot\boldsymbol{\sigma}_p) \tag{6}$$

After eliminating $\mathbf{v}_p$, the conservation of mass eq 1 becomes

$$\frac{\partial\phi}{\partial t} = -\mathbf{v}\cdot\nabla\phi + \nabla\cdot[\zeta^{-1}(\nabla\pi_\phi - \nabla\cdot\boldsymbol{\sigma}_p)] \tag{7}$$

where $\phi\zeta = \lambda$. The appearance of polymer stress in the concentration equation can be understood by writing eq 7 in the following form:

$$\frac{\partial\phi}{\partial t} = -\nabla\cdot\mathbf{j}_\phi \tag{8}$$

where $\mathbf{j}_\phi$ is the polymer current given by

$$\mathbf{j}_\phi = \phi\mathbf{v} + \zeta^{-1}(-\nabla\pi_\phi + \nabla\cdot\boldsymbol{\sigma}_p) \tag{9}$$

In addition to the convective current and diffusive current caused by osmotic forces, there exists a polymer current caused by an inhomogeneous polymer elastic stress.

The equation of motion for the total fluid velocity $\mathbf{v}$ is obtained by combining eqs 3 and 6

$$\varrho\frac{\partial\mathbf{v}}{\partial t} = \eta_s\nabla^2\mathbf{v} + \nabla\cdot\boldsymbol{\sigma}_p - \nabla\pi_\phi - \nabla p \tag{10}$$

We assume incompressibility of the polymer solution, which implies $\nabla\cdot\mathbf{v} = 0$. This means that the velocity field in an incompressible fluid is transverse. We define a transverse projection operator $\mathbf{T}$, and since $\mathbf{v}$ is transverse $\mathbf{T}\cdot\mathbf{v} = \mathbf{v}$. Operating on the velocity eq 10 with this projection operator, we get

$$\varrho\frac{\partial\mathbf{v}}{\partial t} = \eta_s\nabla^2\mathbf{v} + \mathbf{T}\cdot(\nabla\cdot\boldsymbol{\sigma}_p) \tag{11}$$

Equations 7 and 11 are the key results obtained from the two-fluid model. In order to use these equations to study fluctuations in polymer solutions, we must put them in canonical Langevin form and add stochastic forces. This will be the subject of the following section.

IV. Langevin Equations

We are interested in formulating a description of fluctuations in polymer solutions under shear flow. A fluctuating system can be described by Langevin's stochastic theory. This theory is based on the assumption that there exists a set of variables with time scales for their variations much longer than that of the remaining degree of freedom. One then writes Langevin equations of motion for these slow variables with the effects of fast processes (such as microscopic collisions) represented by random force terms. For a set of slow variables A_i, the generalized Langevin equations[14] have the following form:

$$\frac{\partial A_i}{\partial t} = -K_{ij}\frac{\delta F}{\delta A_j^*} + \frac{\partial K_{ij}}{\partial A_j^*} + \theta_i \tag{12}$$

where

$$K_{ij} = M_{ij} + L_{ij} \tag{13}$$

One recognizes the factor $\partial F/\partial A_j^*$ as the conjugate variable of A_j. M_{ij} arises from Poisson bracket coupling, which conserves energy and satisfies the symmetry relation $M_{ij} = -M_{ji}^*$ (here the asterisk denotes complex conjugate). L_{ij} is the Onsager coupling, satisfying the Onsager reciprocal relation $L_{ij} = L_{ji}^*$. The terms containing $\mathbf{L}$ are dissipative. In general, M_{ij} and L_{ij} can be operators. θ_i is a random force term, which represents the effect of fast processes. The correlations between random noise satisfy the fluctuation–dissipation relation:

$$\langle\theta_i(t)\theta_j^*(t')\rangle = 2L_{ij}k_BT\delta(t-t') \tag{14}$$

In the previous section, we used the two-fluid model to derive equations of motion for polymer concentration and velocity. To describe fluctuations in polymer solutions, these equations must be converted to the canonical Langevin form as in eq 12. To do so, a new variable, which is conjugate to polymer stress $\boldsymbol{\sigma}_p$, must be introduced. The conjugate variable for stress is usually a strain variable. In a purely elastic system, strain is given directly by the displacement from equilibrium. However, for a viscoelastic system such as a polymer solution, the definition of strain requires some caution. In a viscoelastic system, strains created by external constraints are constantly dissipated through relaxation. For example, sufficiently long after the application of step strain, both strain and stress would have relaxed to zero in a polymer liquid. Following Leonov,[15] we introduce an elastic (recoverable) strain $\mathbf{W}$. The elastic strain $\mathbf{W}$ he defines as the stored strain that

would be recovered if all external constraints were released instantaneously. In the elastic limit of fast deformations, it is reasonable to assume that the stress in a viscoelastic liquid is the same as the stress in a rubber with the given elastic strain. This is in keeping with the usual assumption of irreversible statistical mechanics that the system is in local equilibrium. The polymer stress $\boldsymbol{\sigma}_p$ is then given in terms of the elastic strain, $\mathbf{W}$ (Finger strain), through the relationship[9] of rubber elasticity:

$$\boldsymbol{\sigma}_p = 2\mathbf{W}\cdot\frac{\partial f_{el}}{\partial \mathbf{W}} = \frac{\partial f_{el}}{\partial \mathbf{h}} \tag{15}$$

where f_{el} is the elastic free energy density. The conjugate variable to the stress $\mathbf{h} = {}^1/_2 \ln \mathbf{W}$ is the so-called Hencky tensor in rubber elasticity theory.

The total free energy functional for polymer solutions is taken to be

$$F = F_0[\phi] + F_{el}[\phi,\mathbf{W}] + \int d\mathbf{r}\,\frac{1}{2}\varrho v^2 \tag{16}$$

where F_0 is the usual mixing free energy, a functional of volume fraction:

$$F_0 = \int d\mathbf{r}\,\{f_0(\phi) + \mathscr{L}(\phi)|\nabla\phi|^2\} \tag{17}$$

$$= \frac{1}{2}\int d\mathbf{q}\,\chi^{-1}(q)|\phi(\mathbf{q})|^2 \tag{18}$$

The gradient term reflects the effect of concentration inhomogeneity. For good solvent, $\mathscr{L}(\phi) \sim \phi^{-3/2}$. $\mathbf{X}^{-1}(q)$ is the inverse susceptibility, with $\chi^{-1}(q) = \chi_0^{-1}(1 + \xi^2 q^2)$, where $\chi_0^{-1} = \partial^2 f_0/\partial\phi^2$. ξ is the correlation length of the polymer solution ($\xi \sim a\phi^{-3/4}$ for good solvent).[16] The second term F_{el} is the elastic free energy, which is a functional of both the elastic strain and polymer concentration. The form of F_{el} depends on the specific constitutive model of polymer solutions. This will be given in the next section. The third term is the kinetic energy.

The concentration eq 7 and velocity eq 11 can be converted to a canonical Langevin form by making the following substitutions:

$$\varrho\mathbf{v} = \frac{\delta F}{\delta \mathbf{v}}, \qquad \pi_\phi = \phi\frac{\delta F}{\delta\phi} - \frac{F}{V} \tag{19}$$

and eq 15. One obtains the Langevin equation for polymer concentration:

$$\frac{\partial\phi}{\partial t} = -\frac{1}{\varrho}\frac{\delta F}{\delta \mathbf{v}}\cdot\nabla\phi + \nabla\cdot\left(\frac{\phi}{\zeta}\nabla\frac{\delta F}{\delta\phi}\right) + \nabla\cdot\left[\zeta^{-1}\left(\nabla\mathbf{W}:\frac{\delta F}{\delta \mathbf{W}} - 2\nabla\cdot\left(\mathbf{W}\cdot\frac{\delta F}{\delta \mathbf{W}}\right)\right)\right] + \theta_\phi \tag{20}$$

and the Langevin equation for the velocity:

$$\frac{\partial \mathbf{v}}{\partial t} = \frac{\eta_s}{\varrho^2}\nabla^2\frac{\delta F}{\delta \mathbf{v}} + \frac{2}{\varrho}\mathbf{T}\cdot\left[\nabla\cdot\left(\mathbf{W}\cdot\frac{\delta F}{\delta \mathbf{W}}\right)\right] + \boldsymbol{\theta}_v \tag{21}$$

To complete the set of coupled equations, we also need a Langevin equation for the elastic strain variable $\mathbf{W}$. In general, the equation of motion for $\mathbf{W}$ consists of two parts, representing dissipative and nondissipative processes, respectively. The nondissipative part describes accumulation and convection of strain. It can be derived by considering the evolution of strain in a nondissipative elastic system. For a deformation that causes the point $\mathbf{r}_0$ to move to $\mathbf{r}$, one defines a deformation gradient term

$$\mathbf{E} = \frac{d\mathbf{r}}{d\mathbf{r}_0} \tag{22}$$

and the Finger tensor as

$$\mathbf{W} = \mathbf{E}\cdot\mathbf{E}^T \tag{23}$$

In an inhomogeneous velocity field, the evolution of the deformation tensor $\mathbf{E}$ is $\partial\mathbf{E}/\partial t = \mathbf{E}\cdot\nabla\mathbf{v}$. Using this equation and assuming that the polymer strain tensor is convected by polymer velocity, one arrives at the nondissipative part of the strain equation:[9]

$$\frac{\partial\mathbf{W}}{\partial t} + \mathbf{v}_p\cdot\nabla\mathbf{W} - \nabla\mathbf{v}_p{}^T\cdot\mathbf{W} - \mathbf{W}\cdot\nabla\mathbf{v}_p = \ldots \tag{24}$$

The left-hand side is the so-called upper-convected time derivative of $\mathbf{W}$.

The dissipative part of the strain equation describes strain relaxation. The exact form of strain relaxation is unknown since it is stress relaxations that are usually determined in experiments. However, from the generalized Langevin theory, we know that the dissipation of the Hencky tensor $\mathbf{h}$ (the conjugate variable to stress) must have a dissipative term:

$$\frac{\partial\mathbf{h}}{\partial t} = -L_{hh}\frac{\delta F}{\delta\mathbf{h}} + \frac{\partial L_{hh}}{\partial\mathbf{h}} + \ldots \tag{25}$$

In general, the Onsager coefficient L_{hh} is a function of $\mathbf{h}$. The second term on the right side of the equation must be included to ensure that the fluctuation–dissipation theorem is satisfied.

Here we make the simplest assumption that L_{hh} is independent of the strain $\mathbf{h}$. Although there is no *a priori* reason why this should be the case, the resulting strain equation of motion does have the merit that it is consistent with the generalized Langevin theory, and it describes reasonably well the steady-state shear properties of polymer solutions (cf. Appendix B). By requiring that the predicted zero-shear viscosity of polymer solutions be $\eta_0 = G\tau$ (G is the shear modulus of the polymer solution), one obtains the Onsager coefficient $L_{hh} = (2G\tau)^{-1}$. Hence the dissipation of the Hencky tensor has the form

$$\frac{\partial\mathbf{h}}{\partial t} = -\frac{1}{2G\tau}\frac{\delta F}{\delta\mathbf{h}} + \ldots = -\frac{1}{2G\tau}\boldsymbol{\sigma}_p + \ldots \tag{26}$$

Matrix multiplying both sides by $2\mathbf{W}$, we obtain the form of strain relaxation

$$\frac{\partial\mathbf{W}}{\partial t} = -\frac{1}{G\tau}\mathbf{W}\cdot\boldsymbol{\sigma}_p + \ldots = -\frac{2}{G\tau}\mathbf{W}^2\cdot\frac{\delta F}{\delta\mathbf{W}} + \ldots \tag{27}$$

Combining the nondissipative and dissipative parts in eqs 24 and 27, we obtain the strain equation of motion for polymer solutions:

$$\frac{\partial\mathbf{W}}{\partial t} + \mathbf{v}_p\cdot\nabla\mathbf{W} - \nabla\mathbf{v}_p{}^T\cdot\mathbf{W} - \mathbf{W}\cdot\nabla\mathbf{v}_p = -\frac{2}{G\tau}\mathbf{W}^2\cdot\frac{\delta F}{\delta\mathbf{W}} + \boldsymbol{\theta}_W \tag{28}$$

where $\boldsymbol{\theta}_W$ is thermal noise. The coupling of polymer elastic strain to concentration and velocity is contained in the expression of polymer velocity $\mathbf{v}_p$:

$$\mathbf{v}_p = \frac{1}{\varrho}\frac{\delta F}{\delta \mathbf{v}} + \lambda^{-1}\left[-\theta\nabla\frac{\delta F}{\delta \phi} - \nabla\mathbf{W}:\frac{\delta F}{\delta \mathbf{W}} + 2\nabla\cdot\left(\mathbf{W}\cdot\frac{\delta F}{\delta \mathbf{W}}\right)\right] \tag{29}$$

Equations 20, 21, and 28 form a set of Langevin equations for polymer concentration ϕ, velocity $\mathbf{v}$, and polymer strain $\mathbf{W}$. Supplemented with the free energy functional in eq 16 and a constitutive model (stress–strain relation), it provides a basic framework for studying hydrodynamic motions and fluctuations in polymer solutions.

V. The Elastic Free Energy

To determine the form of the elastic free energy F_{el}, a constitutive model is needed for polymer solutions. The simplest constitutive model[8] is the Maxwell model. It gives a linear stress–strain relationship and is derivable from the Rouse model. However, as the Rouse model neglects both entanglement and hydrodynamic screening effects, this model is not a good description for well-entangled, semidilute polymer solutions. In addition, the Maxwell model predicts neither shear thinning nor second normal stress, both observed in polymer solutions. In this work, we use a constitutive model slightly simplified from that proposed by Doi and Edwards[10] from the reptation theory for entangled polymer systems. A detailed discussion of the model is given in Appendix A. In the simplified form employed here, this model predicts shear thinning and both the first and second normal stress. The derived stress–strain relationship is

$$\boldsymbol{\sigma}_p = G(\phi)\left(\frac{3\mathbf{W}}{I_1} - \mathbf{1}\right) \tag{30}$$

where $\mathbf{1}$ is the unit tensor, $I_1 = \text{trace}(\mathbf{W})$, and $G(\phi)$ is the elastic modulus given by

$$G(\phi) = \frac{\phi kT}{b^3 N_e} \propto \phi^{\alpha} \tag{31}$$

where N_e is the average interval between entanglement points along one chain, b is the monomer size, and $\alpha = 2.25$ for a good solvent. The corresponding elastic free energy density is

$$f_{el}(\phi,\mathbf{W}) = \frac{1}{2}G(\phi)(3\ln I_1 - \ln I_3) \tag{32}$$

where $I_3 = |\mathbf{W}|$ is the determinant of tensor $\mathbf{W}$.

The strain equation of motion for this particular constitutive model is then given by combining eqs 28 and 32:

$$\frac{\partial \mathbf{W}}{\partial t} + \mathbf{v}_p\cdot\nabla\mathbf{W} - \nabla\mathbf{v}_p{}^{T}\cdot\mathbf{W} - \mathbf{W}\cdot\nabla\mathbf{v}_p = -\frac{1}{\tau}\left(\frac{3\mathbf{W}^2}{I_1} - \mathbf{W}\right) + \boldsymbol{\theta}_W \tag{33}$$

However, we must caution here that this strain equation is unlikely to yield a stress equation with a single-exponential stress relaxation.

VI. Fluctuations at Steady-State Shear

In this section, we use the model developed in previous sections to study thermal fluctuations in a polymer solution undergoing steady shear flow. In steady-state shear, a polymer solution is characterized by its concentration ϕ_0, a linear velocity field $\mathbf{v}_0 = \dot{\gamma}y\mathbf{e}_x$ (where $\dot{\gamma}$ is the shear rate and $\mathbf{e}_x$ is the unit vector in the x direction), and a homogeneous strain field $\mathbf{W}_0$. The steady-state strain $\mathbf{W}_0$ is the solution to eq 33 (cf. Appendix B), with the polymer velocity $\mathbf{v}_p$ replaced by $\mathbf{v}_0$ (in the absence of fluctuations, the system is homogeneous and polymers and solvents move at the same velocity in steady shear).

The steady-state shear stress coefficients are shown in Figure 5. The predicted shear viscosity decreases with increasing shear rate (shear thinning), as is commonly observed in polymer solutions. However, our constitutive model also predicted a maximum of shear stress at Deborah number $\dot{\gamma}\tau = 1$. Beyond this point, shear stress falls with increasing shear rate, which implies a flow instability. The existence of such an instability is still a controversial issue at this time. For this reason, only stable flow is considered in this paper ($0 < \dot{\gamma}\tau < 1$). In addition to shear thinning, both first and second normal stresses are predicted in our constitutive model, which is consistent with experimental observations.

Thermal noise causes the system variables (ϕ, $\mathbf{v}$, $\mathbf{W}$) to fluctuate around their steady-state values. These fluctuations are represented by a set of small variables $\delta\phi(r)$, $\delta\mathbf{v}(\mathbf{r})$, and $\delta\mathbf{W}(\mathbf{r})$. It is important to note that fluctuations in polymer solutions are usually accompanied by relative motions between the polymer and the solvent. According to the two-fluid model, the relative velocity between the polymer and the solvent is given by eq 6. In steady state, both the osmotic pressure and the polymer elastic stress are homogeneous. There is no relative motion between polymer and solvent molecules ($\mathbf{v}' = 0$). However, in the presence of thermal fluctuations, concentration waves cause spatial inhomogeneities in osmotic pressure and polymer stress. Consequently, polymer chains move relative to the solvent ($\mathbf{v}' \neq 0$) in the form of a polymer current. It is clear from eq 6 that there are two contributions to the polymer current. One is diffusion, proportional to the gradient of osmotic pressure $-\nabla\pi_\phi$. The other is inhomogeneous polymer stress $\nabla\cdot\boldsymbol{\sigma}_p$. The latter is the origin of stress–concentration coupling.

The evolution of fluctuations is determined by the equations of motion for polymer solutions. For small fluctuations around the steady state we write $\phi = \phi_0 + \delta\phi$, $\mathbf{v} = \mathbf{v}_0 + \delta\mathbf{v}$, and $\mathbf{W} = \mathbf{W}_0 + \delta\mathbf{W}$. Insert these expressions in the equations of motion for polymer concentration (eq 7), velocity (eq 11), and strain (eq 33) and expand to first order in the fluctuating variables to obtain the equations for fluctuations.

The fluctuation in polymer concentration $\delta\phi$ is governed by

$$\frac{\partial\delta\phi}{\partial t} + \mathbf{v}_0\cdot\nabla\delta\phi + \nabla\cdot[\zeta^{-1}(-\nabla\delta\pi_\phi + \nabla\cdot\delta\boldsymbol{\sigma}_p)] = \theta_\phi \tag{34}$$

where $\delta\pi_\phi$ and $\delta\boldsymbol{\sigma}_p$ are deviations in osmotic pressure and polymer stress caused by fluctuations in polymer concentration, velocity, and strain.

The velocity fluctuation $\delta\mathbf{v}$ satisfies the following equation

$$\varrho\frac{\partial\delta\mathbf{v}}{\partial t} - \eta_s\nabla^2\delta\mathbf{v} - \mathbf{T}\cdot(\nabla\cdot\delta\boldsymbol{\sigma}_p) = \boldsymbol{\theta}_v \tag{35}$$

and also the incompressibility condition $\nabla\cdot\delta\mathbf{v} = 0$. However, we will show later that the velocity variables

are fast variables, which will be eliminated by dropping the noise term in the velocity equation.

The equation for the strain fluctuation $\delta\mathbf{W}$ can be derived from eq 33 by writing the strain $\mathbf{W} = \mathbf{W}_0 + \delta\mathbf{W}$ and the polymer velocity $\mathbf{v}_p = \mathbf{v}_0 + \delta\mathbf{v} + \mathbf{v}'$

$$\frac{\partial\delta\mathbf{W}}{\partial t} + \mathbf{v}_0\cdot\nabla\delta\mathbf{W} - \nabla\mathbf{v}_0{}^T\cdot\delta\mathbf{W} - \delta\mathbf{W}\cdot\nabla\mathbf{v}_0 - \nabla(\mathbf{v}' + \delta\mathbf{v})^T\cdot \mathbf{W}_0 - \mathbf{W}_0\cdot\nabla(\mathbf{v}' + \delta\mathbf{v}) + \delta\left\{\frac{1}{\tau}\left[\frac{3\mathbf{W}^2}{I_1} - \mathbf{W}\right]\right\} = \boldsymbol{\theta}_W \quad (36)$$

where the relative velocity is $\mathbf{v}' = \lambda^{-1}(-\nabla\delta\pi_\phi + \nabla\cdot\delta\boldsymbol{\sigma}_p)$.

Equations 34–36 form a complete description of fluctuations in a sheared polymer solution. To simplify the following discussion, we write these equations in terms of a simple general form:

$$\frac{\partial\mathbf{A}}{\partial t} + \mathbf{v}_0\cdot\nabla\mathbf{A} + \boldsymbol{\Lambda}\cdot\mathbf{A} = \theta_A \quad (37)$$

where $\mathbf{A}$ is defined as a vector with its components given by the fluctuating variables $\mathbf{A} \equiv (\delta\phi, \delta\mathbf{v}, \delta\mathbf{W})$. The coefficient matrix $\boldsymbol{\Lambda}$ is given by expanding eqs 34–36 and using the following expressions for $\delta\pi_\phi$ and $\delta\boldsymbol{\sigma}_p$:

$$\delta\pi_\phi = \phi\frac{\partial^2 f}{\partial\phi^2}\delta\phi + \left(\phi\frac{\partial^2 f}{\partial\phi\partial\mathbf{W}} - \frac{\partial f}{\partial\mathbf{W}}\right):\delta\mathbf{W} \quad (38)$$

and

$$\delta\boldsymbol{\sigma}_p = G'(\phi_0)\left(\frac{3\mathbf{W}_0}{I_1} - \mathbf{1}\right)\delta\phi + 3G(\phi_0)\left(\frac{\delta\mathbf{W}}{I_1} - \frac{\mathbf{W}_0}{I_1{}^2}\sum_k \delta\mathbf{W}_{kk}\right) \quad (39)$$

A quantitative measure of concentration fluctuations is given by the structure factor $\langle\delta\phi(\mathbf{q})\delta\phi(-\mathbf{q})\rangle$ (where the $\langle\ \rangle$ denotes thermal average). This quantity is directly measured in scattering experiments.[3,4] To calculate the structure factor in our theory, we introduce a correlation matrix $S_{ij} \equiv (2\pi)^3\langle A_i A_j{}^*\rangle/V$. V is the volume of the system. The structure factor is one of the elements of this matrix. The correlation matrix S_{ij} satisfies the following equation, derived from the fluctuation eq 37

$$\frac{\partial\mathbf{S}}{\partial t} + \mathbf{v}_0\cdot\nabla\mathbf{S} + \boldsymbol{\Lambda}\cdot\mathbf{S} + \mathbf{S}\cdot\boldsymbol{\Lambda}^T = 2\mathbf{L} \quad (40)$$

where $\boldsymbol{\Lambda}$ is the matrix of Onsager coefficients. In deriving this equation, we have used the fluctuation–dissipation theorem (eqs C3–5). In steady state $\partial\mathbf{S}/\partial t = 0$. Take the Fourier transform of eq 40 to arrive at

$$\dot\gamma q_x\frac{\partial\mathbf{S}}{\partial q_y} = \boldsymbol{\Lambda}\cdot\mathbf{S} + \mathbf{S}\cdot\boldsymbol{\Lambda}^T - 2\mathbf{L} \quad (41)$$

Equation 41 is a coupled set of linear differential equations that can be solved numerically. The numerical procedure used to obtain polymer structure factor $S(\mathbf{q})$ is discussed in section VIII.

The Onsager matrix $\mathbf{L}$ is extracted from the canonical Langevin form of the equations of motion (eqs 20, 21, and 28) in section IV. L_{ij} is the coefficient in front of $-\delta F/\delta A_j{}^*$ in the equation for dA_i/dt. We have verified that the Onsager reciprocal relations are satisfied.

VII. Fluctuations under Time-Dependent Flow Conditions

In the previous section, we derived equations for fluctuations in a polymer solution under steady shear conditions. Often flow situations are not steady but time-dependent. It is important to understand the dynamical response of fluctuations under time-dependent flow conditions. For this purpose, we propose a test flow condition in which a small oscillatory shear is superimposed on a steady shear. The oscillation is in the same direction as the steady shear. This will create a small change in the fluctuations, which can be measured in a scattering experiment. The modification to fluctuations contains two components, one in-phase and the other out-of-phase with the oscillation. The variation of these components with the frequency of oscillation provides valuable information on the dynamical modes of fluctuations.

The general equation for polymer structure factor $\mathbf{S}$ is eq 40. For our test flow condition, the velocity field is given by $\mathbf{v} = \mathbf{v}_0 + \Delta\mathbf{v}$. Here $\mathbf{v}_0 = \dot\gamma y\bar{\mathbf{e}}_x$ is the steady shear part, and $\Delta\mathbf{v} = \Delta\dot\gamma\exp(-i\omega t)y\bar{\mathbf{e}}_x$ is the oscillatory part.[17] ω and $\Delta\dot\gamma$ are the frequency and amplitude of the oscillation, respectively. The small-oscillation assumption implies that $\Delta\dot\gamma \ll \dot\gamma$. In eq 40 we denote the steady-state quantities as $\mathbf{S}_0$, $\boldsymbol{\Lambda}_0$, and $\mathbf{L}_0$. These quantities satisfy the steady-state equation:

$$\mathbf{v}_0\cdot\nabla\mathbf{S}_0 + \boldsymbol{\Lambda}_0\cdot\mathbf{S}_0 + \mathbf{S}_0\cdot\boldsymbol{\Lambda}_0{}^T = 2\mathbf{L}_0 \quad (42)$$

With the addition of the small oscillation, an oscillatory component is added to the structure factor $\mathbf{S} = \mathbf{S}_0 + \Delta\mathbf{S}\exp(-i\omega t)$. (Here we only keep terms to order $\Delta\dot\gamma$.) The polymer strain and the matrices $\mathbf{L}$ and $\boldsymbol{\Lambda}$ are also modified: $\mathbf{W} = \mathbf{W}_0 + \Delta\mathbf{W}\exp(-i\omega t)$, $\boldsymbol{\Lambda} = \boldsymbol{\Lambda}_0 + \Delta\boldsymbol{\Lambda}\exp(-i\omega t)$, and $\mathbf{L} = \mathbf{L}_0 + \Delta\mathbf{L}\exp(-i\omega t)$. The oscillatory part of the strain $\Delta\mathbf{W}$ can be calculated by expanding the constitutive equation 33 around the steady-state solution. Subsequently $\Delta\mathbf{L}$ and $\Delta\boldsymbol{\Lambda}$ are determined by linear expansion of $\mathbf{L}$ and $\boldsymbol{\Lambda}$. The equation for $\Delta\mathbf{S}$ is derived by inserting these expressions in eq 40 and expanding, making use of the steady state eq 42. After Fourier transform, we get

$$\dot\gamma q_x\frac{\partial\Delta\mathbf{S}}{\partial q_y} = \boldsymbol{\Lambda}_0\cdot\Delta\mathbf{S} + \Delta\mathbf{S}\cdot\boldsymbol{\Lambda}_0{}^T - i\omega\Delta\mathbf{S} - 2\left(\Delta L + \frac{\Delta\dot\gamma}{\dot\gamma}\mathbf{L}_0\right) + \left(\Delta\boldsymbol{\Lambda} + \frac{\Delta\dot\gamma}{\dot\gamma}\boldsymbol{\Lambda}_0\right)\cdot\mathbf{S}_0 + \mathbf{S}_0\cdot\left(\Delta\boldsymbol{\Lambda}^T + \frac{\Delta\dot\gamma}{\dot\gamma}\boldsymbol{\Lambda}_0{}^T\right) \quad (43)$$

This is a set of linear differential equations, which can be solved numerically. In general, the solution to this equation is complex. The real part of $\Delta\mathbf{S}$ is in phase with the oscillation, and the imaginary part is out-of-phase.

VIII. Elimination of the Velocity Variable

We now show that the velocity $\mathbf{v}$ is a fast variable, which can be eliminated from the set of long-lived variables. It is convenient to write the velocity eq 35 in terms of its Fourier transform, since the transverse projection operator $\mathbf{T}$ has the simple form in Fourier space $\mathbf{T} = \mathbf{1} - \mathbf{e}_q\mathbf{e}_q$ ($\mathbf{1}$ is the unit tensor, and $\mathbf{e}_q$ is the unit vector in the $\mathbf{q}$ direction). In terms of the Fourier component of the velocity fluctuation $\delta\mathbf{v}(\mathbf{q})$, we have

$$\varrho\frac{\partial\delta\mathbf{v}}{\partial t} + \eta_s q^2\delta\mathbf{v} + i\mathbf{q}\cdot\delta\boldsymbol{\sigma}_p\cdot(\mathbf{1} - \mathbf{e}_q\mathbf{e}_q) = \boldsymbol{\theta}_v \quad (44)$$

The fluctuation in velocity $\delta\mathbf{v}$ relaxes at a rate $\Gamma_v = \nu q^2$, where $\nu = \eta/\varrho$ is the kinematic viscosity of the solvent.

For polymer concentration fluctuation, $\delta\phi$, the relaxation rate is $\Gamma_\phi = D_\phi q^2$, where D_ϕ is the concentration diffusion constant. The ratio of concentration and velocity relaxation rates is

$$\frac{\Gamma_v}{\Gamma_\phi} = \frac{\nu}{D_\phi} \tag{45}$$

A typical diffusion constant for polymer in semidilute solutions is of order $D_\phi \sim 10^{-10}$ cm^2/s.[3] For most organic solvents, the order of magnitude of kinematic viscosity is $\nu \sim 10^{-2}$ cm^2/s. Thus $\Gamma_v/\Gamma_\phi \sim 10^8 \gg 1$. $\delta\phi$ relaxes at a much slower rate than $\delta\mathbf{v}$. The strain relaxation occurs roughly at a rate of $1/\tau$. For wavenumbers typical of light scattering in polymer solutions ($D_\phi q^2 \sim 1/\tau$), this is also much slower than the velocity relaxations.

We then proceed to eliminate the fast velocity variable according to the general principle discussed in Appendix C. The velocity equation is eliminated and the velocity fluctuation $\delta\mathbf{v}$ is slaved to $\delta\phi$ and $\delta\mathbf{W}$ according to the relation

$$\delta\mathbf{v} = -\frac{\mathrm{i}}{\eta_s \mathrm{q}}\mathbf{e}_q\cdot\delta\boldsymbol{\sigma}_p\cdot(\mathbf{1} - \mathbf{e}_q\mathbf{e}_q) \tag{46}$$

where $\delta\boldsymbol{\sigma}_p$ is given by eq 39. The K matrix for the remaining variables $\delta\phi$ and $\delta\mathbf{W}$ is modified according to the rule

$$K_{ij}' = K_{ij} - \frac{K_{iv}K_{vj}}{K_{vv}} \tag{47}$$

where i and j represent $\delta\phi$ or the components of tensor $\delta\mathbf{W}$.

IX. Numerical Solutions for the Polymer Structure Factor

In this section, we discuss the numerical procedure used in solving eq 41. It is convenient to first reduce this equation to a dimensionless form appropriate for numerical integration. For this purpose, we introduce the following quantities.

(1) A normalized concentration fluctuation $\overline{\delta\phi} = \delta\phi/\phi_0$. The correlation matrix $\mathbf{S}$ is then redefined, with $\delta\phi$ replaced by $\overline{\delta\phi}$.

(2) A normalized correlation matrix $\bar{\mathbf{S}}(\mathbf{q}) = \mathbf{S}(\mathbf{q})/S_0$, where $S_0 = \chi\phi_0^{-2}$. With this normalization, $\bar{\mathbf{S}}(0) = 1$ in the absence of shear.

(3) The Deborah number $\kappa = \dot{\gamma}\tau$.

(4) A normalized wave vector $\bar{\mathbf{q}} = \mathbf{q}/q^*$, where q^* is a characteristic wave vector defined by $Dq^{*2} = \tau^{-1}$, and $D = \lambda^{-1}\phi_0^2\chi^{-1}$ is the diffusion constant.

Using these normalized quantities, eq 41 can be written in a dimensionless form

$$\kappa\bar{q}_x\frac{\partial\bar{\mathbf{S}}}{\partial\bar{q}_y} = \bar{\mathbf{\Lambda}}\cdot\bar{\mathbf{S}} + \bar{\mathbf{S}}\cdot\bar{\mathbf{\Lambda}}^{\mathrm{T}} - 2\bar{\mathbf{L}} \tag{48}$$

where $\bar{\mathbf{L}} = \tau\phi_0^2\chi^{-1}\mathbf{L}$ and $\bar{\mathbf{\Lambda}} = \tau\mathbf{\Lambda}$.

The detailed expressions for $\bar{\mathbf{L}}$ and $\bar{\mathbf{\Lambda}}$ are rather cumbersome and will not be written out explicitly here. In evaluating these two matrices, four additional parameters appear:

$$\alpha = \frac{\partial(\ln G)}{\partial(\ln\phi)} \qquad \beta = \frac{\partial(\ln\tau)}{\partial(\ln\phi)} \qquad \epsilon = G\chi\phi_0^{-2}$$
$$\bar{\xi} = \xi q^* \tag{49}$$

It is clear from the definition that $G \sim \phi^\alpha$ and $\tau \sim \phi^\beta$. α and β describe, respectively, the sensitivity of the elastic modulus G and relaxation time τ with regard to variations of polymer concentration. For good solvents, it is known both experimentally and theoretically that $\alpha \approx 2.25$ and $\beta \approx 1.5$.[18] These values are used in the present work. ϵ is a measure of the system's elasticity. It gives the ratio of typical elastic stress and the osmotic stress in a polymer solution. For calculations presented in this paper, we chose $\epsilon = 0.33$ and $\bar{\xi} = 0.3$, appropriate for a typical experimental situation.[3,8]

Equation 48 is a set of stiff differential equations. A stiff equation is an equation with wide separation between the longest and the shortest relaxation times. Numerically, stiff differential equations can be integrated using the backward differentiation formulae (BDF) method.[19] For eq 48, the integration is done in the following way. For a fixed positive q_x, we first choose a large positive q_{y0} where the integration is to be initialized, with an arbitrary initial value of S_{ij} (chosen to be $S_{ij} = 0$ here). Using the BDF routine, we then integrate the equations in the direction of decreasing q_y. If the integration is started at a sufficiently large q_{y0}, the integrated value of $\mathbf{S}(\mathbf{q})$ quickly converges to a steady solution that is independent of the initial condition.

Equation 48 can be integrated for arbitrary wave vector $\mathbf{q}$. Experimental measurements of $S(\mathbf{q})$ have been made for $\mathbf{q}$ in the $q_xq_y^3$ and $q_xq_z^4$ planes. To compare with experiments, we present here numerical solutions of $S(\mathbf{q})$ for wave vectors in these two planes.

To calculate $\mathbf{S}(q_x,q_y)$, we set $q_z = 0$ in eq 48. With the velocity variable eliminated, only five fluctuating variables are coupled: $\overline{\delta\phi}$, δW_{xx}, δW_{yy}, δW_{zz}, and δW_{xy}. In eq 37, this means that vector $\mathbf{A}$ has five components. There are then 15 independent correlation functions in the matrix $\mathbf{S}$ (25 total correlation functions, with 10 given by symmetry $S_{ij} = S_{ji}^*$). Solving for $\mathbf{S}(q_x,q_y)$ thus involves integrating 15 coupled differential equations. The numerical solutions of $S_{\phi\phi}(q_x,q_y)$ for four different Deborah numbers are shown in Figure 2 in contour plots.

Similarly, $\mathbf{S}(q_x,q_z)$ can be calculated by setting $q_y = 0$ in eq 48. Here there are seven coupled fluctuating variables: $\overline{\delta\phi}$, δW_{xx}, δW_{yy}, δW_{zz}, δW_{xy}, δW_{xz}, and δW_{yz}. There are seven components to $\mathbf{A}$, and 28 independent correlation functions in the $\mathbf{S}$ matrix ($49 - 21 = 28$). Figure 3 shows the contour plots of the computed $S_{\phi\phi}(q_x,q_z)$.

The equation for the oscillatory contribution $\Delta\mathbf{S}$ (eq 43) is integrated using the same numerical scheme. Here we first write this equation in terms of its real and imaginary components separately and arrive at a coupled set of 30 equations. These equations are integrated using the BDF routine and results are shown in Figure 4. Instead of showing the contour plot of $\Delta S_{\phi\phi}$, it is more instructive to trace the frequency dependence of $\Delta S_{\phi\phi}$ at a fixed wave vector $\mathbf{q}$. These results will be discussed in the following section.

X. Discussion and Conclusions

The computed polymer structure factor $S_{\phi\phi}(\mathbf{q})$, as shown in contour plots in Figures 2 and 3, can be

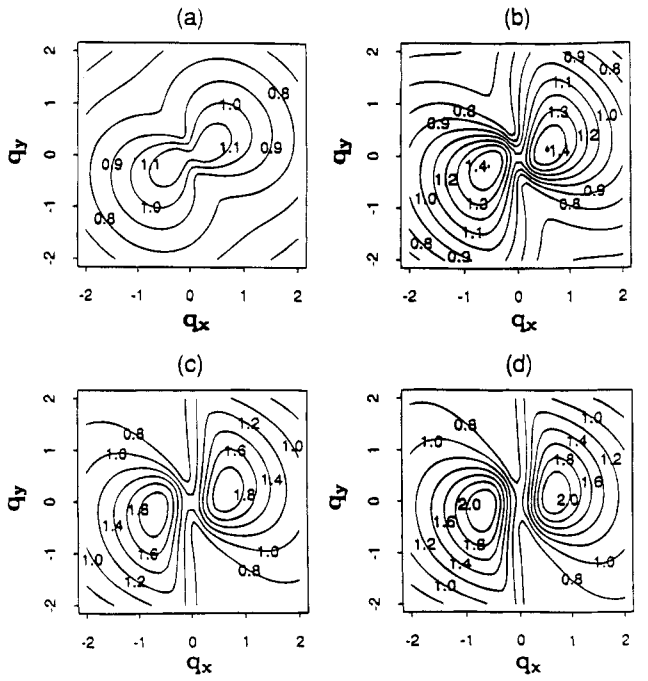

Figure 2. Contour plots of polymer structure factor in the flow-gradient plane $\bar{S}_{\phi\phi}(q_x,q_y)$. The Deborah numbers are (a) 0.2, (b) 0.5, (c) 0.8, and (d) 1.0. The wavenumber q is given in units of q^*.

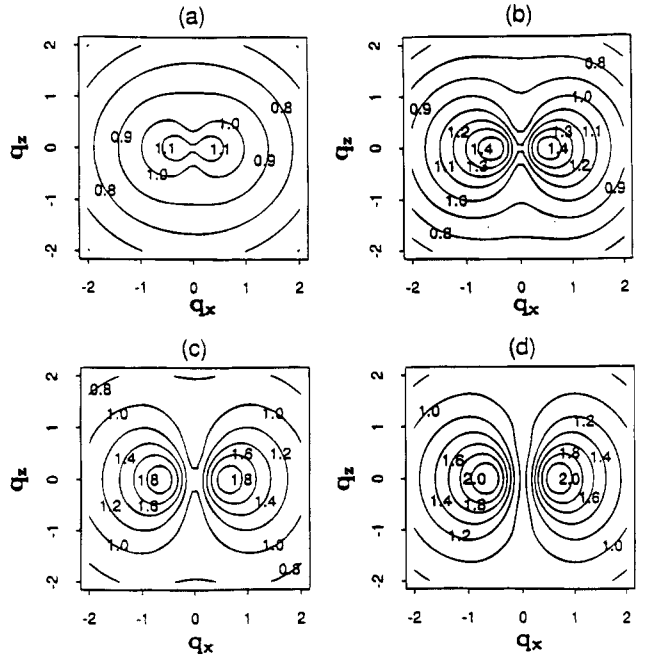

Figure 3. Contour plots of polymer structure factor in the flow-vorticity plane $\bar{S}_{\phi\phi}(q_x,q_z)$. The Deborah numbers are (a) 0.2, (b) 0.5, (c) 0.8, and (d) 1.0.

compared directly with light scattering measurements. Because of the various approximations made in the present model, we will only discuss the qualitative aspect of our results. The structure factor for wave vectors in the flow-vorticity plane (q_xq_z), $\bar{S}_{\phi\phi}(q_x,q_z)$, is shown in Figure 3. In the absence of shear, the scattering is isotropic, and the contour plot of the structure factor is a sequence of circles with the strongest scattering at the origin $\bar{S}_{\phi\phi}(0) = 1$. At low shear (Figure 3a), the scattering is enhanced for waves with $\mathbf{q}$ in the flow direction. The strongest scattering occurs roughly at wavenumber $q_x \simeq 0.5q^*$, creating two symmetric scattering peaks on the q_x axes (the peak wavenumber increases only weakly with increasing shear rate). Along the vorticity direction, the enhancement of scattering is relatively small. The resulting pattern is anisotropic with a characteristic "butterfly" shape. The wings of the "butterfly" are aligned in the flow direction (q_x), and there is a dark streak along the vorticity direction (q_z). As the shear rate increases, the total scattering intensity increases. In addition, the "wings" of the "butterfly" become wider as the dark streak is gradually narrowed (Figure 3b–d). Qualitatively, these results agree well with the light scattering measurements by Hashimoto *et al.*[4]

The structure factor in the flow-gradient (q_xq_y) plane, $\bar{S}_{\phi\phi}(q_x,q_y)$, is shown in Figure 2. Similar to the structure factor in the flow-vorticity plane (Figure 3), these patterns also have an anisotropic "butterfly" shape, with increasingly strong scattering as the shear rate increases. However, at low shear, the "wings" of the "butterfly" are aligned along the $q_x = q_y$ direction (the origin of which is discussed in section II). In addition, as the shear rate increases, the "butterfly" pattern rotates in a clockwise manner. At the highest shear rate studied here ($\kappa = 1$), the alignment of the two peaks is rotated to a nearly horizontal direction, parallel to the direction of flow (Figure 2d). These results are in accord with the experimental observation of Wu *et al.*[3]

The rotation of the "butterfly" pattern in the flow-gradient scattering plane is a consequence of affine convection of concentration waves. In a shear field $\mathbf{v} = \dot{\gamma}y\mathbf{e}_x$, a concentration wave with wave vector $\mathbf{q}_0 = (q_x, q_y, q_z)$ initially is convected to a new wave vector $\mathbf{q} = (q_x, q_y - \dot{\gamma}q_xt, q_z)$ at time t later. Thus all waves are affinely convected from the first quadrant to the fourth quadrant along the gradient direction. For example, a wave born with a wave vector along the $q_x = q_y$ line, which is strongly enhanced by the mechanism discussed in section II, may, within its lifetime, be convected so that its $\mathbf{q}$ points toward the flow direction. The scattering intensity at a certain $\mathbf{q}$ is thus determined by the superposition of waves convected to this wave vector, averaged over time. With increasing strong shear, waves are rotated more before they diffuse away, leading to the overall rotation of the scattering patterns.

The scattering pattern in the flow-vorticity plane does not rotate with increasing shear because convection by a shear field $\mathbf{v} = \dot{\gamma}y\mathbf{e}_x$ only influences the q_y component of the wave vector. More importantly, the scattering pattern reflects the symmetry between waves in the q_xq_z plane. In addition to the usual inversion symmetry between $\mathbf{q}$ and $-\mathbf{q}$, there exists also a reflection symmetry between $\mathbf{q}_+ = (q_x, q_z)$ and $\mathbf{q}_- = (q_x, -q_z)$ because z is a neutral direction in the problem.

When a small oscillatory shear is added to the steady shear, the change in the scattering function is calculated and shown in Figure 4. In general, the change in the structure factor reflects the strength of coupling between concentration wave and the imposed oscillation. ΔS acts like a response function. The strongest response occurs when the oscillation frequency matches the relaxation rate of the dominant normal mode of fluctuations. In the absence of convection, the plot of $\Delta S_{\phi\phi}$ vs frequency of oscillation should show individual peaks around each normal mode of concentration–strain fluctuation. Convection tends to mix these normal modes. As a consequence, these peaks are usually smeared out. Nevertheless, if the frequency range between the fast and slow modes is sufficiently large, it is possible to identify regions (in the q space) where fluctuations are dominated by fast or slow modes.

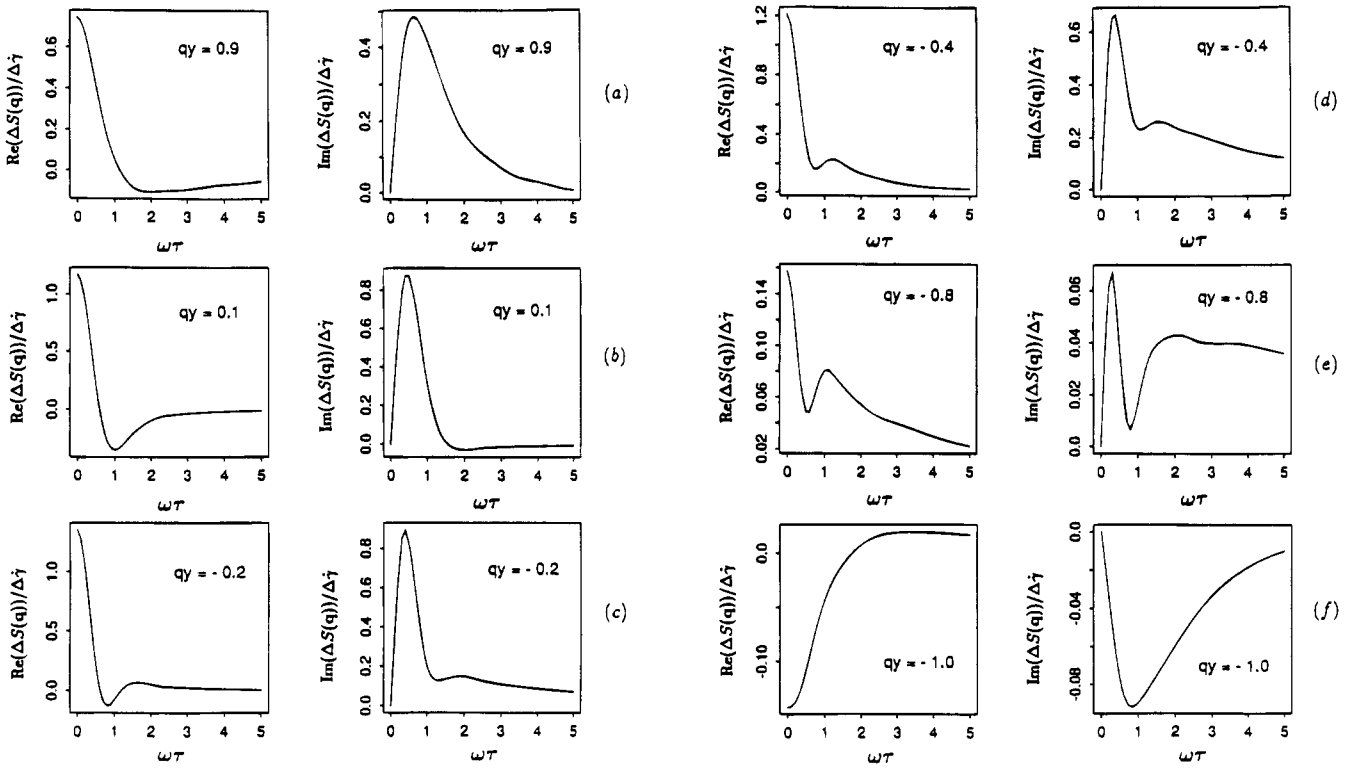

Figure 4. Change in the steady-state structure factor when a small oscillatory shear is added to the steady shear. Here the normalized real and imaginary parts of $\Delta S/\Delta\dot{\gamma}$ are plotted against the reduced frequency $\omega\tau$ at a certain wave vector $\mathbf{q}$. The Deborah number for steady shear is 0.5. q_x is fixed at $q_x = 0.5$. q_y is (a) 0.9, (b) 0.2, (c) −0.2, (d) −0.4, (e) −0.8, and (f) −1.0.

We have plotted $\Delta S_{\phi\phi}$ vs the reduced frequency $\omega\tau$ for Deborah number 0.5 and for six different wave vectors. (Here we use the normalized quantity $\Delta S_{\phi\phi}/\Delta\dot{\gamma}$.) We chose a fixed $q_x = 0.5$, and six values of q_y. At zero frequency, the imaginary part $\mathrm{Im}(\Delta S(0))$ is always zero. The real part $\mathrm{Re}(\Delta S(0))$ could be either positive or negative. A positive $\mathrm{Re}(\Delta S(0))$ indicates enhanced scattering with increasing shear, whereas a negative $\mathrm{Re}(\Delta S(0))$ is a sign of diminished scattering with increasing shear at a certain wave vector $\mathbf{q}$. We see that $\mathrm{Re}(\Delta S(0))$ is positive for all $\mathbf{q}$ in Figure 4 except $q_y = -1.0$ (Figure 4f). This point is in the dark streak region, which shows weaker scattering with increasing shear.

It is interesting to follow the variations of the $\Delta S-\omega\tau$ curve as we go from the first quadrant, pass the peak, enter the fourth quadrant, and finally reach the region of the dark streak. Since the general trend is the same for both the real and the imaginary parts of δS, we shall only discuss the $\mathrm{Im}(\Delta S)-\omega\tau$ curve. For $q_y = 0.9$, the curve has a wide distribution with its peak located around $\omega\tau \sim 1$. For $q_y = 0.1$, which is roughly at the peak position of the steady-state scattering, the distribution is much narrower with a higher peak shifted to lower frequency (Figure 4b). This is an indication that slow modes become dominant over fast modes at this wave vector $\mathbf{q}$. The decay of concentration waves is overall slower, giving rise to strongly enhanced fluctuations. As we go down in q_y and enter the fourth quadrant, a second peak, located at a higher frequency range, gradually appears (Figure 4c–e). At the same time, the first peak in the lower frequency range is lowered and the entire distribution is widened. Presumably, this is because the fast modes are becoming more important in the dissipation of concentration waves. The enhancement in scattering becomes weaker until finally in the dark streak region, the scattering is actually diminished by shear.

In conclusion, we have developed a phenomenological model to study fluctuations in sheared polymer solutions. The numerically calculated polymer structure factor agrees qualitatively with light scattering measurements. However, the model as is presently formulated is limited in several aspects, and improvement must be made before quantitative predictions may be directly compared with experiments. One important issue here is the characterization of the strained state of polymer solutions. In this work, we have used a single stress tensor variable $\boldsymbol{\sigma}_p$ (and its conjugate strain variable $\mathbf{h}$) for this purpose. It is known from the reptation theory that under strain, tube segments along one chain are deformed differently depending on their relative positions.[20] A more complete description of the strained state would then require a tensor variable for each tube segment. Secondly, we have assumed a one-to-one correspondence between the stress and strain variables (see eq 30). For many practical situations, this condition must also be relaxed for a more realistic description of the memory effects in viscoelastic materials. Finally, a better constitutive model is needed which describes well the various rheological properties of polymer solutions, and the issue of mechanical instabilities must be resolved.

Appendix A: Derivations of the Constitutive Equations

In an entangled polymer system, the motion of polymer chains is restricted by the topological constraint which forbids them from crossing through one another. This effect is often represented by a tubelike region around each polymer chain. The tube diameter a is related to the degree of entanglement in the system. It is independent of chain length for sufficiently long chains.

For our purpose, it is convenient to subdivide the tube into a sequence of segments, each represented by a vector $\mathbf{r}$. In the unstrained state, the segment length is chosen to be the same as the tube diameter a, and the orientations of tube segments are totally uncorrelated. The tube can then be treated as a random walk of freely jointed tube segments.

Using the tube model, Doi and Edwards[10] derived the stress induced by a step strain, $\mathbf{r}_0 \rightarrow \mathbf{r} = \mathbf{E}\cdot\mathbf{r}_0$, where $\mathbf{r}_0$ and $\mathbf{r}$ are tube segment vectors before and after the deformation, and $\mathbf{E}$ is the deformation tensor. The derived stress tensor is

$$\boldsymbol{\sigma}_p = 3kTc\mathcal{N}_0\frac{1}{\langle r\rangle}\left\langle\frac{\mathbf{rr}}{r}\right\rangle \tag{A1}$$

where c is the number of chains per unit volume and $\mathcal{N}_0$ is the average number of tube segments per chain in equilibrium.

In evaluating the averages in the above expression, Doi and Edwards used the so-called independent alignment approximation, which amounts to the substitution

$$\frac{1}{\langle r\rangle}\left\langle\frac{\mathbf{rr}}{r}\right\rangle \simeq \left\langle\frac{\mathbf{rr}}{r^2}\right\rangle \tag{A2}$$

Here, for the simplification it affords, we make the approximation

$$\frac{1}{\langle r\rangle}\left\langle\frac{\mathbf{rr}}{r}\right\rangle \simeq \frac{\langle\mathbf{rr}\rangle}{\langle r^2\rangle} \tag{A3}$$

The stress tensor is then given by

$$\boldsymbol{\sigma} = 3G\frac{\langle\mathbf{rr}\rangle}{\mathrm{trace}\langle\mathbf{rr}\rangle} \tag{A4}$$

where G is the elastic modulus defined as

$$G \equiv kTc\mathcal{N}_0 = \frac{kT\phi}{N_e v_p} \tag{A5}$$

ϕ is the monomer volume fraction, N_e is the degree of polymerization between entanglements, and v_p is the monomer volume.

We now establish the connection between the second moment of tube segment vector $\langle\mathbf{rr}\rangle$ and the finger tensor $\mathbf{W}$. For a subchain in an undeformed tube segment, the equilibrium distribution function is assumed to be Gaussian:

$$P(\mathbf{r}_0) = \left(\frac{3}{2\pi a_0^2}\right)^{3/2}\exp\left(-\frac{3}{2a_0^2}r_0^2\right) \tag{A6}$$

For affine deformations, the probability distribution function after the deformation is related to that before the deformation by the relation

$$P(\mathbf{r}_0)\,d\mathbf{r}_0 = P(\mathbf{r})\,d\mathbf{r} \tag{A7}$$

The finger tensor is defined as

$$\mathbf{W} \equiv \mathbf{E}\cdot\mathbf{E}^T \tag{A8}$$

Note that

$$d\mathbf{r} = |\mathbf{W}|^{3/2}\,d\mathbf{r}_0 \tag{A9}$$

where $|\mathbf{W}|$ is the determinant of tensor $\mathbf{W}$, and

$$r_0^2 = \mathbf{W}^{-1}:\mathbf{rr} \tag{A10}$$

Thus, we obtain

$$P(\mathbf{r}) = \left(\frac{3}{2\pi a^2|\mathbf{W}|}\right)^{3/2}\exp\left(-\frac{3}{2a^2}\mathbf{W}^{-1}:\mathbf{rr}\right) \tag{A11}$$

One may then find $\langle\mathbf{rr}\rangle$ by evaluating the Gaussian integral

$$\langle\mathbf{rr}\rangle = \int d\mathbf{r}\,\mathbf{rr}P(\mathbf{r}) \tag{A12}$$

which gives

$$\langle\mathbf{rr}\rangle = \frac{a^2}{3}\mathbf{W} \quad \text{and} \quad \mathrm{trace}\langle\mathbf{rr}\rangle = \frac{a^2}{3}\mathrm{trace}(\mathbf{W}) = \frac{a^2}{3}I_1 \tag{A13}$$

Inserting these expressions into eq A4, we obtain the stress–strain relationship

$$\boldsymbol{\sigma} = G\frac{3\mathbf{W}}{I_1} \tag{A14}$$

In terms of the deviatoric stress $\boldsymbol{\sigma}_p$,

$$\boldsymbol{\sigma}_p = G\left(\frac{3\mathbf{W}}{I_1} - 1\right) \tag{A15}$$

The corresponding elastic energy is obtained by recalling that (eq 15)

$$\boldsymbol{\sigma}_p = 2\mathbf{W}\cdot\frac{\partial f_{el}}{\partial\mathbf{W}} \tag{A16}$$

We get

$$f_{el}(\phi,\mathbf{W}) = \frac{1}{2}G(\phi)(3\ln I_1 - \ln I_3) \tag{A17}$$

Appendix B: Descriptions of Steady-State Shear

In this appendix, we discuss the steady-state shear properties of the constitutive eqs 33 and 30. For simple shear, the velocity field is $\mathbf{v}_0 = \dot\gamma y\mathbf{e}_x$, where $\dot\gamma$ is the shear rate. In steady state, $\partial\mathbf{W}/\partial t = 0$, and $\nabla\mathbf{W} = 0$ because strain in homogeneous. Setting $\mathbf{v}_p = \mathbf{v}_0$ in eq 33, one gets

$$-\nabla\mathbf{v}_0^T\cdot\mathbf{W} - \mathbf{W}\cdot\nabla\mathbf{v}_0 = -\frac{1}{\tau}\left(\frac{3\mathbf{W}^2}{I_1} - \mathbf{W}\right) \tag{B1}$$

Here the noise term is ignored. Writing out each component of this tensorial equation, one obtains a set of coupled nonlinear equations for W_{xx}, W_{yy}, W_{zz}, and W_{xy}

$$3(W_{xx}^2 + W_{xy}^2)/I_1 - W_{xx} = 2\dot\gamma\tau W_{xy} \tag{B2}$$

$$3(W_{xy}^2 + W_{yy}^2)/I_1 - W_{yy} = 0 \tag{B3}$$

$$3W_{zz}^2/I_1 - W_{zz} = 0 \tag{B4}$$

$$3(W_{xx} + W_{yy})W_{xy}/I_1 - W_{xy} = \dot\gamma\tau W_{yy} \tag{B5}$$

where $I_1 = W_{xx} + W_{yy} + W_{zz}$. These equations have an analytical solution $\mathbf{W}_0$.

$$W_{0xx} = \frac{1 + 2(\dot\gamma\tau)^2}{1 + (\dot\gamma\tau)^2} \qquad W_{0yy} = \frac{1}{1 + (\dot\gamma\tau)^2} \tag{B6}$$

$$W_{0zz} = 1 \qquad W_{0xy} = \frac{\dot\gamma\tau}{1 + (\dot\gamma\tau)^2} \tag{B7}$$

The stress tensor $\boldsymbol{\sigma}_p$ is then given by the stress–strain relation eq 30. In terms of the shear viscosity η and

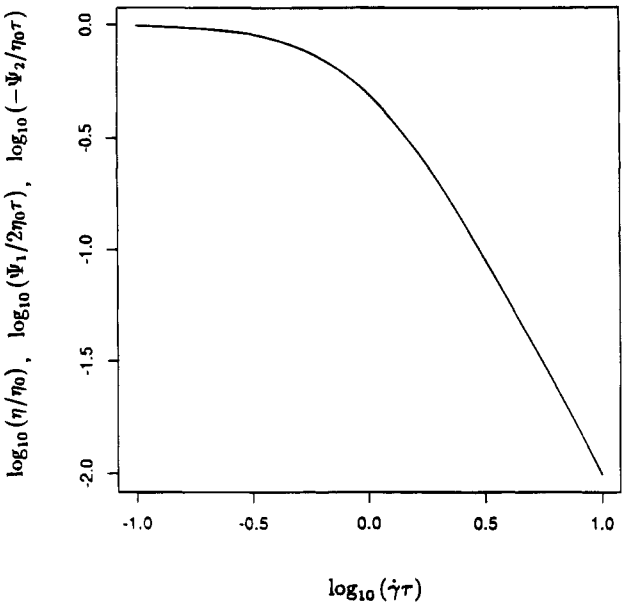

Figure 5. Variations of stress coefficients with shear rate. Here the three stress coefficients follow the same shear-thinning curve.

first and second normal stress coefficients Ψ_1 and Ψ_2, the predictions of the constitutive model are

$$\frac{\eta}{\eta_0} = \frac{1}{1+(\dot\gamma\tau)^2} \qquad \eta_0 = G\tau \tag{B8}$$

$$\frac{\Psi_1}{2\eta_0\tau} = \frac{1}{1+(\dot\gamma\tau)^2} \qquad \frac{\Psi_2}{\eta_0\tau} = -\frac{1}{1+(\dot\gamma\tau)^2} \tag{B9}$$

The variation of stress coefficients with shear rate is plotted in Figure 5. Normalized as η/η_0, $\Psi_1/2\eta_0\tau$, and $-\Psi_2/\eta_0\tau$, all three stress coefficients follow the same shear-thinning curve. At zero shear, $\Psi_2/\Psi_1 = -0.5$. The magnitude of this ratio is bigger than typically observed in experiments (~ -0.2).[9] Hence the second normal stress is overestimated in this simple model. The predicted shear stress σ_{xy} has a maximum at $\dot\gamma\tau = 1$. Beyond this point, shear stress decreases with increasing shear rate. This indicates a mechanical instability.

Appendix C: Elimination of Fast Variables

Consider a set of coupled Langevin equations for two variables A and B:

$$\frac{\partial A}{\partial t} = -K_{AA}\frac{\delta F}{\delta A} - K_{AB}\alpha B + \theta_A \tag{C1}$$

$$\frac{\partial B}{\partial t} = -K_{BA}\frac{\delta F}{\delta A} - K_{BB}\alpha B + \theta_B \tag{C2}$$

we have taken $\delta F/\delta B = \alpha B$ for simplicity. θ_A and θ_B are stochastic variables which represent the effects of fast processes in the system. Their ensemble averages are zero and their cross-correlations satisfy the fluctuation–dissipation relations

$$\langle\theta_A(t)\theta_A^*(t')\rangle = 2L_{AA}k_BT\delta(t-t') \tag{C3}$$

$$\langle\theta_B(t)\theta_B^*(t')\rangle = 2L_{BB}k_BT\delta(t-t') \tag{C4}$$

$$\langle\theta_A(t)\theta_B^*(t')\rangle = 2L_{AB}k_BT\delta(t-t') \tag{C5}$$

where the superscript asterisk denotes complex conjugate. Onsager's reciprocal relation states that $L_{AB} = L_{BA}^*$ for dissipative coupling. The nondissipative coupling satisfies $M_{AB} = -M_{BA}^*$.

Define a time $T_B = (\alpha K_{BB})^{-1}$ and assume that T_B is independent of B. Equation C2 can then be integrated to give

$$B(t) = -\int_{-\infty}^{t} dt' \left[K_{BA}\frac{\delta F}{\delta A}\right] \exp\left[-\frac{t-t'}{T_B}\right] + \int_{-\infty}^{t} dt'\, \theta_B(t') \exp\left[-\frac{t-t'}{T_B}\right] \tag{C6}$$

Suppose B is a fast variable with a short relaxation time T_B. The first integral in the above expression may be evaluated by treating the slowly varying part (bracketed) as constant. This gives

$$B(t) \simeq -K_{BA}\frac{\delta F}{\delta A}T_B + \int_{-\infty}^{t} dt'\, \theta_B(t') \exp\left[-\frac{t-t'}{T_B}\right] \tag{C7}$$

Inserting this expression for B in eq C1, we get

$$\frac{\partial A}{\partial t} = -\left(K_{AA} - \frac{K_{AB}K_{BA}}{K_{BB}}\right)\frac{\delta F}{\delta A} + \left(\theta_A - K_{AB}\alpha\int_{-\infty}^{t} dt'\, \theta_B(t') \exp\left[-\frac{t-t'}{T_B}\right]\right) \tag{C8}$$

defining

$$K_{AA}' \equiv K_{AA} - \frac{K_{AB}K_{BA}}{K_{BB}} \tag{C9}$$

$$\theta_A' \equiv \theta_A - K_{AB}\alpha\int_{-\infty}^{t} dt'\, \theta_B(t') \exp\left[-\frac{t-t'}{T_B}\right] \tag{C10}$$

We obtain the new Langevin equation for A after eliminating the fast variable B,

$$\frac{\partial A}{\partial t} = -K_{AA}'\frac{\delta F}{\delta A} + \theta_A' \tag{C11}$$

It can be shown that the fluctuation–dissipation relation is preserved for the new Langevin equation. Inserting θ_A' from eq C10 into the left hand side expression and evaluating the integrals in the expansion, one gets

$$\langle\theta_A'(t)\theta_A'(t')\rangle = \left[2L_{AA} - \left(\frac{K_{AB}K_{BA}}{K_{BB}} + \frac{K_{AB}^*K_{BA}}{K_{BB}^*}\right)\right]k_BT\delta(t-t') \tag{C12}$$

where we have used the relationship that for sufficiently small T,

$$\frac{1}{2T}\exp\left[-\frac{|t'-t|}{T}\right] \simeq \delta(t-t') \tag{C13}$$

The new Onsager coefficient is

$$L_{AB}' = L_{AB} - \frac{1}{2}\left(\frac{K_{AB}K_{BA}}{K_{BB}} + \frac{K_{AB}^*K_{BA}^*}{K_{BB}^*}\right) \tag{C14}$$

which satisfies the Onsager reciprocal relation $L_{AB}' = L_{BA}'$.

In general, for Langevin equations

$$\frac{\partial A_i}{\partial t} = -K_{ij}\frac{\delta F}{\delta A_j} - K_{iB}\alpha B = \theta_{A_i} \tag{C15}$$

$$\frac{\partial B}{\partial t} = -K_{Bi}\frac{\delta F}{\delta A_i} - K_{BB}\alpha B + \theta_B \tag{C16}$$

eliminating fast variable B leads to a new set of Langevin equations

$$\frac{\partial A_i}{\partial t} = -K_{ij}'\frac{\delta F}{\delta A_j} + \theta_{A_i}' \tag{C17}$$

with the new K matrix given by

$$K_{ij}' = K_{ij} - \frac{K_{iB}K_{Bj}}{K_{BB}} \tag{C18}$$

References and Notes

(1) Ver Strate, G.; Philippoff, W. *Polym. Lett.* **1974**, *12*, 267. Rangel-Nafaile, C.; Metzner, A. B.; Wissburn, K. F. *Macromolecules* **1984**, *17*, 1187.
(2) Helfand, E.; Fredrickson, G. H. *Phys. Rev. Lett.* **1989**, *62*, 2468.
(3) Wu, X. L.; Pine, D. J.; Dixon, P. K. *Phys. Rev. Let.* **1991**, *68*, 2408.
(4) Hashimoto, T.; Fujioka, K. *J. Phys. Soc. Jpn.* **1991**, *60*, 356. Hashimoto, T.; Kume, T. *J. Phys. Soc. Jpn.* **1992**, *61*, 1839. Moses, E.; Kume, T.; Hashimoto, T., to be published.
(5) Nakatani, A. I.; Takahashi, Y.; Han, C. C. *Polym. Commun.* **1989**, *30*, 43. Hammouda, B.; Nakatani, A. I.; Waldow, D. A.; Han, C. C. *Macromolecules* **1992**, *25*, 2903.
(6) Brochard, F.; de Gennes, P.-G. *Macromolecules* **1977**, *10*, 1157.
(7) Onuki, A. *J. Phys. Soc. Jpn.* **1990**, *59*, 3423.
(8) Milner, S. T. *Phys. Rev. E* **1993**, *48*, 3674.
(9) Larson, R. G. *Constitutive Equations for Polymer Melts and Solutions*; Butterworths: Boston, 1988.
(10) Doi, M.; Edwards, S. F. *The Theory of Polymer Dynamics*; Clarendon Press: Oxford, 1986.
(11) Doi, M. In *Dynamics and Patterns in Complex Fluids: New Aspects of the Physics–Chemistry Interface*; Onuki, A., Kawasaki, K., Eds.; Springer Proceedings in Physics; Springer-Verlag: Berlin, 1990; Vol. 52.
(12) The expression for λ can be deduced by a blob argument.[16] The friction per unity volume of blobs, λ, is given by the concentration of blobs, $1/\xi^3$, times the Stokes friction on a single blob, $\sim\eta_s\xi$. It has been assumed that the hydrodynamic and excluded volume screening lengths are proportional.
(13) In defining a Reynolds number, one must take care to determine what the correct distance scale is. For the present problem there are two distance scales: the gap in the viscometer, L; and the wavelength of the fluctuation under consideration, $2\pi/q$. If the fluctuation produces a fluid velocity change of magnitude $\delta v(q)$, then the convective term is of order $\varrho\dot{\gamma}Lq\delta v$ while the dissipative term is of order $\eta_s q^2\delta v$, with ratio that is small.
(14) Mori, H.; Fujisaka, H. *Prog. Theor. Phys.* **1973**, *49*, 764. Kawasaki, K. *J. Phys. A* **1973**, *6*, 1289.
(15) Leonov, A. I. *J. Non-Newtonian Fluid Mech.* **1992**, *42*, 323.
(16) de Gennes, P.-G. *Scaling Concepts in Polymer Physics*, 2nd ed.; Cornell University Press: Ithaca, NY, 1985.
(17) Experimentally, this is achieved by oscillating one of the two plates. In general, the distribution of induced velocity field in the fluid is sinusoidal. It may be approximated by a linear field only when the gap between the two plates is sufficiently narrow: $h \ll (2\nu/\omega)^{1/2}$. See: Landau, L. D.; Lifshitz, E. M. *Fluid Mechanics*; Pergamon Press: New York, 1987; p 88.
(18) Pearson, D. S. In *Rubber Chem. Technol.* **1987**, *60*, 439.
(19) Hall, G.; Watt, J. M., Eds. *Modern Numerical Methods for Ordinary Differential Equations*; Clarendon Press: Oxford, 1976. Kahaner, D.; Moler, C.; Nash, S. *Numerical Methods and Software*; Prentice-Hall: Englewood Cliffs, NJ, 1988.
(20) Doi, M. *J. Phys. Soc. Jpn.* **1982**, *51*, 3672.

MA946067M